

Experimental and Quantum-chemical Studies on Dissociative Photoionization

Dissociation photoionization of molecules is a common photochemical process upon excitation of vacuum ultraviolet and has played a crucial part in ion chemistry in the atmosphere. Important information as ionic structures, ionization mechanisms and energetic for ions, molecules and radicals have been explored with various photoionization methods and theoretical calculations. In this report, we describe the new results of two atmospherically important compounds upon dissociative photoionization to show the advantages of combining photoionization mass spectrometry with quantum chemical calculations.

Vacuum ultraviolet (VUV) photoionization mass spectrometry (PIMS) is a powerful and well-developed technique for investigating dissociation processes of molecules upon ionization. This method can provide information of photoionization dynamics and energetics for ions, neutrals and radicals through appropriate thermochemical cycles. With synchrotron radiation as a VUV ionization source, applications of PIMS technique in studies of thermochemical data and dissociative photoionization become more important and popular.

Theoretical calculations produce thermochemical data that allow one to assess experimental data and to predict possible dissociation mechanisms. The Gaussian-2 (G2) and Gaussian-3 (G3) methods predict energies accurately; the average magnitudes of deviation of calculated G2 and G3 values from experimental values are 0.07 and 0.04 eV, respectively, for 146 well established ionization energies and electron affinities of molecules containing elements in the first and second rows of the periodic chart.

In this highlight, we report the dissociative photoionization of CH_2Cl_2 and CH_2Br_2 both experimentally and theoretically. We performed photoionization mass-spectrometric measurements with a molecular beam/quadrupole mass spectrometer system on the 1-m Seya-Namioka beamline and undertook theoretical calculations of molecular energies with the G2 and G3 methods.

Ionization of CH_2Cl_2 has been investigated in both gaseous and condensed phases with various techniques, including PIMS, PES, and matrix-isolation IR-UV spectroscopy. Potential-energy curves near the ionization threshold for CH_2Cl_2^+ isomers were also explored with quantum-chemical calculations, but dissociative photoionization channels of CH_2Cl_2 at greater ionization energies are little investigated, either experimentally or theoretically.

Three major fragment ions CH_2Cl^+ , CHCl^+ and CCl^+ were observed in the dissociative photoionization of CH_2Cl_2 in a region ~ 11 – 24 eV. The photoionization efficiency (PIE) curves near the threshold regions of CH_2Cl_2^+ , CH_2Cl^+ , CHCl^+ , and CCl^+ , shown in Figs. 1(a)–(d), were used to determine ionization energy (IE) of CH_2Cl_2 and appearance energy (AE) of each fragment ion. The IE of CH_2Cl_2 was determined to be 11.315 ± 0.004 eV from the first distinct maximum in the first derivative of the PIE curve. This IE value agrees satisfactorily with a recent value of 11.32 ± 0.01 eV. AE values for CH_2Cl^+ , CHCl^+ and CCl^+ were determined to be 12.08 ± 0.02 , 12.46 ± 0.01 , and 15.96 ± 0.03 eV, respectively. Our AE value of 12.08 ± 0.02 eV for CH_2Cl^+ agrees with EI values of 12.10 and 12.1 ± 0.1 eV, but is slightly smaller than a previous PI value of 12.14 ± 0.02 eV; a small discrepancy probably reflects that the effect of hot bands and ion-molecular reaction observed in the previous work are negligible under supersonic expansion conditions in our experiments. The AE

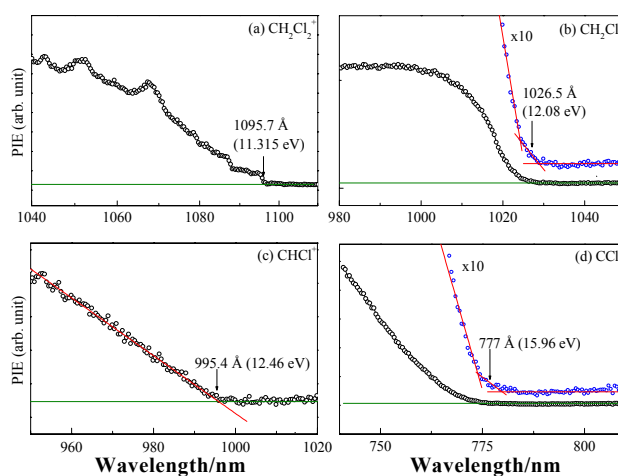


Fig. 1: Photoionization efficiency curves of CH_2Cl_2 and fragment ions CH_2Cl^+ , CHCl^+ , and CCl^+ , together with their respectively fitted lines near the threshold region.

values of 12.46 ± 0.01 and 15.96 ± 0.03 eV for CHCl^+ and CCl^+ respectively are reported for the first time.

We calculated G2 energies and enthalpies and derived enthalpies of formation ($\Delta H_{f,0}^\circ$ and $\Delta H_{f,298}^\circ$) and ionization energies for CH_2Cl_2 and species pertinent to this work. Predicted values of $\Delta H_{f,0}^\circ$ and $\Delta H_{f,298}^\circ$ for CH_2Cl_2 , CH_2Cl_2^+ , CH_2Cl , CH_2Cl^+ , CHCl_2 , CHCl_2^+ , HCl , HCl^+ , Cl_2 , and Cl_2^+ agree with existing literature values within 2 kcal mol⁻¹. Larger discrepancies for CHCl , CHCl^+ , CCl , and CCl^+ might reflect experimental uncertainties. The differences of IE between experiments and calculations are within ± 0.12 eV for all species except CHCl and CCl ; the large difference of 0.34 eV for CHCl indicates a large uncertainty of the previously reported $\Delta H_{f,298}^\circ(\text{CHCl}^+)$.

Dissociative photoionization channels for formation of CH_2Cl^+ , CHCl^+ and CCl^+ are proposed based on comparison of determined AE values and predicted energies. Table 1 lists experimental and calculated dissociation energies (E_d) of four possible dissociation channels, and reaction barriers, $V(\text{G2})$, of two dissociation channels with barriers. The principal dissociative process is direct breakage of the C–Cl bond to form $\text{CH}_2\text{Cl}^+ + \text{Cl}$; at greater energies formation of CHCl^+ takes place via the $\text{CHCl}^+ + \text{HCl}$ channel. Their experimental E_d values of 0.77 and 1.15 eV agree satisfactorily with $E_d(\text{G2})$ values of 0.75 and 1.13 eV, respectively. As the $\text{CHCl}^+ + \text{HCl}$ channel likely involves structural change, relative energies of a feasible dissociation mechanism are shown in Fig. 2. CH_2Cl_2^+ undergoes a three-center elimination via a transition structure TS1 to form CHCl^+ and HCl ; the energy of TS1 is above that of CH_2Cl_2^+ , but below the dissociation energy. Based on the experimental results, we derived $\Delta H_{f,0}^\circ(\text{CHCl}^+) = 288.0 \pm 0.7$ kcal mol⁻¹, $\Delta H_{f,0}^\circ(\text{CH}_2\text{Cl}_2^+) = 239.5 \pm 0.5$ kcal mol⁻¹, $\text{IE}(\text{CHCl}) = 9.12 \pm 0.12$ eV, and $\text{IE}(\text{CH}_2\text{Cl}_2) = 11.315 \pm 0.004$ eV.

Table 1: Comparison of experimental and calculated dissociation energies (E_d) or reaction barriers $V(\text{G2})$ of possible dissociative ionization channels of CH_2Cl_2^+ .

Dissociation channels	$E_d(\text{this work})^a$ (eV)	$E_d(\text{G2})^b$ (eV)	$V(\text{G2})$ (eV)	ΔE_d^c (eV)
1 $\text{CH}_2\text{Cl}_2^+ \rightarrow \text{CH}_2\text{Cl}^+ + \text{Cl}$	0.77 ± 0.02	0.75		0.02
2 $\text{CH}_2\text{Cl}_2^+ \rightarrow \text{CHCl}^+ + \text{HCl}$	1.15 ± 0.01	1.13		0.02
3a $\text{CH}_2\text{Cl}_2^+ \rightarrow \text{CCl}^+ + \text{H}_2 + \text{Cl}$	4.65 ± 0.03	4.00	4.85	-0.20
3b $\rightarrow \text{CCl}^+ + \text{HCl} + \text{H}$		4.07	4.61	0.04

^a Dissociation energy $E_d = \text{AE} - \text{IE}$; $\text{IE} = 11.315$ eV from this work.

^b Dissociation energy $E_d(\text{G2})$ calculated from $E_0(\text{G2})$ energies.

^c $\Delta E_d = E_d(\text{this work}) - E_d(\text{G2})$ or $E_d(\text{this work}) - V(\text{G2})$, if $V(\text{G2})$ is applicable.

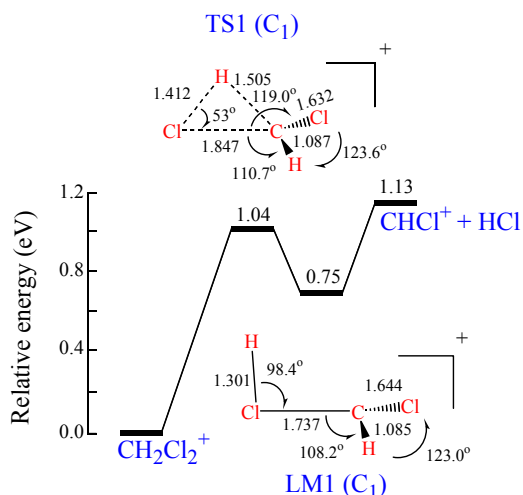


Fig. 2: Theoretical predictions of relative energies for the dissociation channel $\text{CH}_2\text{Cl}_2^+ \rightarrow \text{CHCl}^+ + \text{HCl}$.

For formation of CCl^+ near the threshold, two channels $\text{CH}_2\text{Cl}_2^+ \rightarrow \text{CCl}^+ + \text{H}_2 + \text{Cl}$ and $\text{CCl}^+ + \text{HCl} + \text{H}$ are energetically accessible. Although the experimental E_d value of 4.65 eV conforms satisfactorily to the calculated reaction barrier of 4.61 eV for the $\text{CCl}^+ + \text{HCl} + \text{H}$ channel, it is also within uncertainties of the barrier of 4.85 eV calculated for the $\text{CCl}^+ + \text{H}_2 + \text{Cl}$ channel. Based on anti-correlation between branching ratios of CH_2Cl^+ and CCl^+ above 16 eV, we proposed that formation of CCl^+ near the threshold may proceed via the $\text{CCl}^+ + \text{HCl} + \text{H}$ channel rather than $\text{CCl}^+ + \text{H}_2 + \text{Cl}$ channel, but at greater energies the latter dominates.

CH_2Br_2 is an important substance that contains bromine and destroys ozone because it contributes up to 20% of Br atoms released into the upper troposphere. It has wide use as a reagent for cyclopropanation, but the main anthropogenic sources of CH_2Br_2 originate from its use in fire extinguishers and as a fumigant. Ultraviolet absorption spectra and photoelectron spectra of CH_2Br_2 are well characterized, but only limited experimental work on the dissociative photoionization properties of CH_2Br_2 and the corresponding thermochemical data for associated fragments are reported in the literature.

We measured photoionization efficiency spectra of various fragment ions and undertook associated theoretical calculations with both G2 and G3 methods. The spin-orbit correction is excluded in G2 theory, but found to be important for molecules containing third-row atoms. The G3 method includes experimental spin-orbit corrections for atomic species. Because basis sets for bromine-containing species are lacking from standard G3

calculations, we employed basis sets reported by Curtiss.

An adiabatic ionization energy of 10.25 ± 0.02 eV was determined from a small step-like feature near the ionization threshold of CH_2Br_2 , in agreement with predictions of 10.26 and 10.25 eV with G2 and G3 methods, respectively. For CH_2Br^+ , determined AE of 11.22 ± 0.02 eV agrees with the onset of the third ionic state of CH_2Br_2^+ and a band at 11.3 eV in the photoelectron spectrum. An accurate AE for CH_2Br^+ was unreported in the literature due to severe interference of formation of an ion pair. In contrast, no signal results from interference observed in our spectrum. Considering the quality of our data, our value of 11.22 eV is expected to be more accurate than existing literature values. AE values of 12.59, 15.31, 15.42, and 16.80 eV for CHBr^+ , Br^+ , CBr^+ and CH_2^+ , respectively, determined with the PI method are reported for the first time.

Table 2 lists experimental AE values of fragment ions and reaction energies ΔE calculated for possible dissociative photoionization channels for six fragment ions. Based on comparison of determined appearance energies and predicted energies, six dissociative photoionization channels $\text{CH}_2\text{Br}_2^+ \rightarrow \text{CH}_2\text{Br}^+ + \text{Br}$, $\text{CHBr}^+ + \text{HBr}$, $\text{CHBr}^+ + \text{H} + \text{Br}$, $\text{CHBr}_2^+ + \text{H}$, $\text{Br}^+ + \text{CH}_2\text{Br}$, $\text{CBr}^+ + \text{H}_2 + \text{Br}$ are proposed. In addition, $\Delta H_{f,298}^\circ(\text{CHBr}^+) \leq 300.7 \pm 1.5$ kcal mol⁻¹ is derived experimentally; the IE of CHBr is thus derived to be $\leq 9.17 \pm 0.23$ eV. Literature values for $\Delta H_{f,298}^\circ(\text{CBr}^+) = 362.5$ kcal mol⁻¹ and IE of 10.43 eV for CBr are revised to be less than 332 kcal mol⁻¹ and 9.11 eV, respectively.

Table 2. Experimental appearance energies (AE/eV) of fragment ions and calculated reaction energies (ΔE /eV) for various dissociative photoionization channels of CH_2Br_2 .

Fragment ions	Proposed neutral	AE (expt.)	$\Delta E(\text{G2})^a$	$\Delta E(\text{G3})$
CH_2Br^+	Br	11.22	11.44 (11.28)	11.39
CHBr^+	HBr	12.59	12.37	12.40
	H + Br		16.25 (16.09)	16.16
CHBr_2^+	H	12.64	12.21	12.23
Br^+	CH_2Br	15.31	14.71 (14.53)	14.62
CBr^+	$\text{H}_2 + \text{Br}$	15.42	14.76 (14.60)	14.77
	HBr + H		15.41	15.51
CH_2^+	Br + Br	16.80	16.84 (16.52)	16.63
	Br_2		14.65	14.65

^a $\Delta E(\text{G2})$ values with spin-orbit corrections of Br and Br^+ are listed in parentheses.

In summary, we have shown the advantages of combining photoionization mass spectroscopy and theoretical calculations with the G2 and G3 methods in studying dissociative photoionization of molecular beam cooled CH_2Cl_2 and CH_2Br_2 molecules upon ionization in the region $\sim 10\text{--}24$ eV. Assessment of accuracies of predicted thermochemical properties with G2 and G3 methods in the literature focus mainly on molecules containing atoms in the first and second rows; predictions of accurate enthalpies of formation and IE for polyatomic species containing third-row atoms are more challenging because of increased configuration interaction and spin-orbit effects. Our work also shows that predicted enthalpies of formation for bromine-containing species at the G3 level are typically closer to experimental values than those at the G2 level. Last, the author would like to thank the National Science Council of Taiwan for financial support.

BEAMLINE

04B Seya beamline

EXPERIMENTAL STATION

Molecular Beam/Threshold Photoelectron-photoion Coincidence end station

AUTHOR

S.-Y. Chiang
National Synchrotron Radiation Research Center,
Hsinchu, Taiwan

PUBLICATIONS

- S.-Y. Chiang, M. Bahou, K. Sankaran, Y.-P. Lee, H.-F. Lu, and M.-D. Su, *Journal of Chemical Physics* **118**, 62 (2003).
- S.-Y. Chiang, Y.-S. Fang, K. Sankaran, and Y.-P. Lee, *Journal of Chemical Physics* **120**, 3270 (2004).

CONTACT E-MAIL

schiang@nsrrc.org.tw